

Probing high-energy electronic excitations using inelastic neutron scattering

Young-June Kim,^{1,*} A. P. Sorini,² C. Stock,³ T. G. Perring,⁴ J. van den Brink,⁵ and T. P. Devereaux^{2,6}

¹*Department of Physics, University of Toronto, Toronto, Ontario M5S 1A7, Canada*

²*Stanford Institute for Materials and Energy Science,*

SLAC National Accelerator Laboratory, Menlo Park, California 94025, USA

³*NIST Center for Neutron Research, 100 Bureau Drive, Gaithersburg,*

Maryland 20899, and Indiana University Cyclotron Facility,

2401 Milo B. Sampson Lane, Bloomington, Indiana 47404, USA.

⁴*ISIS Facility, Rutherford Appleton Laboratory, STFC, Chilton,*

Didcot, Oxon OX11 0QX, and Department of Physics and Astronomy,

University College London, Gower Street, London WC1E 6BT, United Kingdom

⁵*Institute for Theoretical Solid State Physics, IFW Dresden, 01171 Dresden, Germany*

⁶*Geballe Laboratory for Advanced Materials, Stanford University, Stanford, California 94305, USA*

(Dated: October 25, 2018)

High-energy, local multiplet excitations of the d-electrons are revealed in our inelastic neutron scattering measurements on the prototype magnetic insulator NiO. These become allowed by the presence of both non-zero crystal field and spin-orbit coupling. The observed excitations are consistent with optical, x-ray, and EELS measurements of d-d excitations. This experiment serves as a proof of principle that high-energy neutron spectroscopy is a reliable and useful technique for probing electronic excitations in systems with significant crystal field and spin-orbit interactions.

PACS numbers: 78.70.Nx, 71.70.Ch, 71.70.Ej

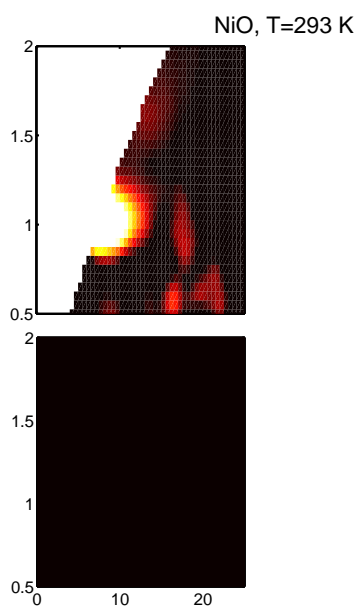
Electrons in strongly correlated systems are characterized by the dual nature of their spatial wave functions; sometimes they are considered localized, but other times delocalized. This dichotomy makes it difficult for traditional band theory to describe physical properties of these scientifically interesting and technologically relevant materials. Often a model based on local interactions, such as a Hubbard Hamiltonian, is used to capture the main physics of these systems, but distilling the numerous interactions present in a condensed matter system into a simple model requires information from experiments. For this reason, various types of electron spectroscopy tools have played significant roles in elucidating various interactions such as crystal field (CF) and spin-orbit (SO) coupling. These include optical, x-ray absorption, photoemission, and electron energy loss spectroscopy (EELS) as well as inelastic x-ray scattering (IXS) in recent years. Here we show that inelastic neutron scattering (INS) can be added to this arsenal of spectroscopic tools for probing *electronic structure* of correlated electron systems.

Neutron spectroscopy has been used to study crystal field splittings in rare-earth insulators [1] and metals [2–5]. With the availability of copious amounts of epithermal neutrons from spallation neutron sources, even intermultiplet transitions in f-electron systems have been observed with INS [6, 7]. Despite earlier theoretical predictions of using INS in studying interband transitions in semiconductors [8], no experimental studies of electronic excitations above 1 eV have been reported to date. Only recently, it was shown that quantitative information above 1 eV can be obtained from direct geometry spectrometers [9]. We note that novel IXS methods have been introduced utilizing either quadrupole tran-

sition matrix element [10, 11] or resonant enhancement in the soft [12, 13] or hard x-ray range [14]. However, such charge-sensitive probes are not ideal for investigating doped Mott insulators, such as cuprate superconductors, because charge carrier contributions dominate the excitation spectrum in the energy range of interest. On the other hand, charge-neutral neutrons do not couple to charge degrees of freedom, and could be very valuable for measuring d-d excitations in such metallic compounds.

In this Letter, as a first step towards this goal, we report our observation of localized d-d excitations in NiO using INS. NiO is a prototypical Mott insulator with a large charge-transfer gap of about 4 eV. This material has been studied extensively using various spectroscopic techniques, and its electronic structure is quite well known. In particular, many novel spectroscopic tools have been recently applied to study NiO d-d excitations as a test case, since the NiO d-d excitations are well characterized [15]. For example, spin-polarized EELS [16], soft x-ray resonant inelastic x-ray scattering (RIXS) [12, 13], hard x-ray RIXS [14], non-resonant IXS [10], and angle-resolved EELS [17] have all been used to detect d-d excitations in NiO. The benefit of studying NiO is that there is no ambiguity with regard to the identification of d-d excitations, thus allowing us to focus on the mechanism of the spectroscopy.

In our INS investigation of NiO, d-d excitations at 1.0 eV and 1.6 eV have been observed, which is the highest energy solid-state excitation observed with INS to date [7]. These transitions occur via magnetic dipole and higher order scattering operators, respectively, giving strong momentum dependence to their spectral weights. We find that either CF splitting or SO coupling is nec-



the exact-diagonalization method to obtain all the eigenstates and eigenenergies.

The eigenstates and energies are used via Fermi's golden rule to obtain the double differential scattering cross-section for unpolarized neutrons as

$$\frac{d\sigma}{d\Omega d\omega} = \frac{k_f}{k_i} \left(\frac{\gamma_n \mu_N}{c} \right)^2 \sum_f |\mathbf{v}|^2 \delta(E_0 + \omega - E_f), \quad (1)$$

where[21]

$$\mathbf{v} = \frac{1}{Q^2} \mathbf{Q} \times \langle \Psi_f | \sum_i e^{i\mathbf{Q}\cdot\mathbf{r}_i} (\mathbf{p}_i + i\mathbf{S}_i \times \mathbf{Q}) | \Psi_0 \rangle, \quad (2)$$

$\mathbf{Q} = \mathbf{k}_i - \mathbf{k}_f$ is the momentum transferred to the electrons, ω is the energy lost by the neutron, and $|\Psi_n\rangle$ and E_n are the states and energies of the electronic system.

The matrix elements in Eq. (2) have a significant dependence on the CF and SO coupling, which can be illustrated by considering the simple limit where $Q \rightarrow 0$ (i.e., the magnetic-dipole approximation). In this approximation the allowed excitations are connected to the ground state by the operator $\mathbf{L} + 2\mathbf{S}$, where \mathbf{L} is the total orbital angular momentum and \mathbf{S} is the total spin. For an isolated non-relativistic atom neither \mathbf{L} nor \mathbf{S} can cause inelastic transitions. However, in the presence of a CF it is well known that the diagonal matrix elements of \mathbf{L} are "quenched". The weight that is removed from these diagonal matrix elements effectively appears in the off-diagonal matrix elements; the presence of a CF allows \mathbf{L} to contribute to the inelastic scattering signal. Similarly, the presence of SO coupling allows \mathbf{S} to contribute to the inelastic signal. The magnetic dipole approximation illustrates the importance of CF and SO.

However, due to neutron kinematics, the momentum transfers at energy-loss appropriate for d-d excitation (on the order of eV) can be large compared to the inverse radial size of the electronic orbitals. Thus the magnetic-dipole approximation is not always valid and the full expression, Eq. (2), must be retained. We will see that the dipolar terms give rise to a non-dispersive intra-multiplet peak at $\omega \approx 10Dq$ which dominates the spectrum at low momentum transfer. For higher momentum transfers, non-dipole excitations appear at higher energies (e.g., 1.6 eV) and eventually dominate the relative scattering intensity. The origin of these peaks can be understood roughly from the Tanabe-Sugano diagram [22] for a d^8 system, which describes the change in multiplet energies as a function of CF strength; transitions from the A_1 octahedral symmetry ground state to the higher energy T_2 and T_1 character states give rise to the spectral peaks at ~ 1.0 eV, and ~ 1.6 eV, respectively. The locations of these peaks are slightly shifted and split by SO coupling. The relative intensity of each peak changes with the magnitude of Q as determined by the matrix-elements of Eq. (2).

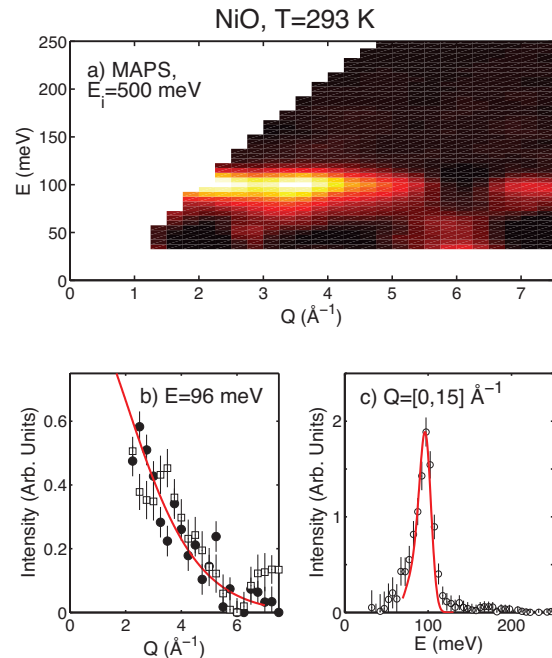


FIG. 3: (Color online) Panel a) illustrates a false contour plot taken on MAPS with the $E_i=500$ meV. b) the intensity of the peak at 96 meV as a function of momentum transfer. The solid and open points are from MARI ($E_i=750$ meV) and MAPS ($E_i=500$ meV) respectively. The solid red line is the free ion Ni^{2+} form factor. c) The momentum integrated scattering and solid line is the calculated density of states from Ref. [23].

In Fig. 1(b) we show the theoretical INS intensity map. The energy integral from 0.9 to 1.25 eV over this map, and the momentum integral for $Q < 20 \text{\AA}^{-1}$, are also shown in Fig. 1(c)-(d) as solid lines. The agreement between theory and experiment is quite good, given that the only adjustable parameter is the overall amplitude. In particular, the momentum dependence shown in Fig. 1(c) suggests that the 1 eV transition occurs via magnetic dipole operator, $\mathbf{L} + 2\mathbf{S}$. The 1.6 eV transition spectral weight is only non-zero in the intermediate Q range, and vanishes both at small and large Q . Since SO coupling in this compound is small, the multiplet splitting due to the SO coupling only shows up as broadening of the 1.6 eV peak.

In addition to the high energy spectrum, we also measured the low energy spin excitation spectrum with $E_i=500$ meV, as shown in Fig. 3. A clear magnon mode is observed around 100 meV, which is the zone boundary spin wave energy. The assignment of this feature is unambiguous in INS. Earlier neutron scattering studies of spin wave dispersion reported that the zone boundary magnon energy is 117 meV [23, 24]. In Fig. 3(b), we plot the intensity as a function of Q . The solid line is the magnetic form factor from the spin angular momentum contribution as tabulated in Ref. [25]. In Fig. 3(c), the

low-Q intensity (integrated up to 5 \AA^{-1} .) is plotted as a function of energy transfer. Since we are using a powder sample, this integration is a quick method to obtain the magnon density of states. We compare this result with the calculated magnon density of states from Hutchings and Samuelsen [23], which agrees very well.

These lower-energy results shed light on understanding excitations observed with different spectroscopic techniques in the energy range of 100-200 meV. As shown in Fig. 3, no significant scattering intensity is observed above the one magnon band up to 250 meV. This should be compared with earlier photon spectroscopy investigation. In optical spectroscopy studies [26], a two-magnon mode at 193 meV was observed with Raman scattering, while an infrared absorption mode due to two-magnon plus phonon was observed at 250 meV. In a recent Ni L_3 -edge RIXS study [18], the excitations at 95 meV and 190 meV were associated with transitions between atomic levels split by an exchange field [27]. We note that “two-magnon” excitations in neutron scattering usually refers to longitudinal spin fluctuations, which usually forms a broad continuum and has very small intensity [28]. The apparent lack of excitations around 190 meV in our INS data clearly illustrates the difference between the “two-magnon” excitations detected with photon spectroscopy and neutron spectroscopy. Further theoretical calculation is necessary to address this issue quantitatively [29].

In summary, we observed d-d excitations of 1 eV and 1.6 eV in NiO using inelastic neutron scattering. Such local multiplet transitions are allowed in the magnetic dipole and higher order channel due to the presence of non-zero crystal field and spin-orbit coupling. The excitation energy matches well with previous experiments, and the momentum dependence of the spectral weight could be well described by the cluster model calculation. Our observation illustrates that inelastic neutron scattering at high energies is a reliable and useful technique for probing electronic excitations in materials with significant crystal field and spin-orbit coupling.

We would like to thank K. Plumb for valuable discussions. Y. K. was supported by Natural Sciences and Engineering Research Council of Canada. A.P.S. and T.P.D. are supported by the U.S. Department of Energy under Contracts No. DE-AC02-76SF00515 and No. DE-FG02-08ER46540 (CMSN).

* Electronic address: yjkim@physics.utoronto.ca

- [1] B. N. Brockhouse, L. N. Becka, K. R. Rao, R. N. Sinclair, and A. D. B. Woods, *J. Phys. Soc. Japan* **17**, **Suppl. B-III**, 63 (1962).
- [2] B. Rainford, K. C. Turberfield, G. Busch, and O. Vogt, *Journal of Physics C: Solid State Physics* **1**, 679 (1968).
- [3] K. C. Turberfield, L. Passell, R. J. Birgeneau, and E. Bucher, *Phys. Rev. Lett.* **25**, 752 (1970).
- [4] R. J. Birgeneau, E. Bucher, L. Passell, and K. C. Turberfield, *Phys. Rev. B* **4**, 718 (1971).
- [5] P. Fulde and M. Loewenhaupt, *Adv. Phys.* **34**, 589 (1985).
- [6] S. M. Shapiro, R. J. Birgeneau, and E. Bucher, *Phys. Rev. Lett.* **34**, 470 (1975).
- [7] A. D. Taylor, R. Osborn, K. A. McEwen, W. G. Stirling, Z. A. Bowden, W. G. Williams, E. Balcar, and S. W. Lovesey, *Phys. Rev. Lett.* **61**, 1309 (1988).
- [8] J. F. Cooke and J. A. Blackman, *Phys. Rev. B* **26**, 4410 (1982).
- [9] C. Stock, R. A. Cowley, J. W. Taylor, and S. M. Bennington, *Phys. Rev. B* **81**, 024303 (2010).
- [10] B. C. Larson, W. Ku, J. Z. Tischler, C.-C. Lee, O. D. Restrepo, A. G. Eguiluz, P. Zschack, and K. D. Finkelstein, *Phys. Rev. Lett.* **99**, 026401 (2007).
- [11] M. W. Haverkort, A. Tanaka, L. H. Tjeng, and G. A. Sawatzky, *Phys. Rev. Lett.* **99**, 257401 (2007).
- [12] G. Ghiringhelli, M. Matsubara, C. Dallera, F. Fracassi, R. Gusmeroli, A. Piazzalunga, A. Tagliaferri, N. B. Brookes, A. Kotani, and L. Braicovich, *Journal of Physics: Condensed Matter* **17**, 5397 (2005).
- [13] S. G. Chiuzbăian, G. Ghiringhelli, C. Dallera, M. Gioni, P. Amann, X. Wang, L. Braicovich, and L. Patthey, *Phys. Rev. Lett.* **95**, 197402 (2005).
- [14] S. Huotari, T. Pytkkanen, G. Vanko, V. R., P. Glatzel, and G. Monaco, *Phys. Rev. B* **78**, 041102 (2008).
- [15] R. Newman and R. M. Chrenko, *Phys. Rev.* **114**, 1507 (1959).
- [16] B. Fromme, C. Koch, R. Deussen, and E. Kisker, *Phys. Rev. Lett.* **75**, 693 (1995).
- [17] F. Müller and S. Hufner, *Phys. Rev. B* **78**, 085438 (2008).
- [18] G. Ghiringhelli, A. Piazzalunga, C. Dallera, T. Schmitt, V. N. Strocov, J. Schlappa, L. Patthey, X. Wang, H. Berger, and M. Gioni, *Phys. Rev. Lett.* **102**, 027401 (2009).
- [19] C. Stock, L. C. Chapon, O. Adamopoulos, A. Lappas, M. Giot, J. W. Taylor, M. A. Green, C. M. Brown, and P. G. Radaelli, *Phys. Rev. Lett.* **103**, 077202 (2009).
- [20] F. de Groot and A. Kotani, *Core Level Spectroscopy of Solids* (CRC Press, Boca Raton, 2008), pp. 119–121.
- [21] E. Balcar and S. W. Lovesey, *Theory of Magnetic Neutron and Photon Scattering* (OUP, Oxford, 1989).
- [22] Y. Tanabe and S. Sugano, *J. Phys. Soc. Jpn.* **9**, 766 (1954).
- [23] M. T. Hutchings and E. J. Samuelsen, *Phys. Rev. B* **6**, 3447 (1972).
- [24] M. T. Hutchings and E. J. Samuelsen, *Solid State Commun.* **9**, 1011 (1971).
- [25] P. J. Brown, in *International tables for crystallography, v. C. Mathematical, physical and chemical tables*, edited by A. Wilson (D. Reidel Pub. Co., Dordrecht, Holland, 1995), pp. 391–399.
- [26] R. E. Dietz, G. I. Parisot, and A. E. Meixner, *Phys. Rev. B* **4**, 2302 (1971).
- [27] F. M. F. de Groot, P. Kuiper, and G. A. Sawatzky, *Phys. Rev. B* **57**, 14584 (1998).
- [28] T. Huberman, R. Coldea, R. A. Cowley, D. A. Tennant, R. L. Leheny, R. J. Christianson, and C. D. Frost, *Phys. Rev. B* **72**, 014413 (2005).
- [29] C.-C. Chen, C. J. Jia, A. F. Kemper, R. R. P. Singh, and T. P. Devereaux, *Phys. Rev. Lett.* **106**, 067002 (2011).
- [30] J. S. Griffith, *The Theory of Transition Metal Ions* (CUP, Cambridge, UK, 1961).

- [31] R. D. Cowan, *The Theory of Atomic Structure and Spectra* (University of California Press, Berkeley, 1981).
- [32] The model is parameterized[30] by the $t_{2g} - e_g$ splitting

$10Dq = 1.05$ eV, the SO coupling [31] $\xi = 0.051$ eV, and the Racah parameters [30, 31] $B = 0.11$ eV and $C = 0.42$ eV.